NeuroImage 202 (2019) 116136

Contents lists available at ScienceDirect

NeuroImage

journal homepage: www.elsevier.com/locate/neuroimage

Ventromedial prefrontal cortex contributes to performance success by controlling reward-driven arousal representation in amygdala

Noriya Watanabe [a,b,c,d,*], Jamil P. Bhanji [a], Hiroki C. Tanabe [c], Mauricio R. Delgado [a,**]

[a] Department of Psychology, Rutgers University, 101 Warren Street, Newark, NJ, 07102, USA
[b] Research Center for Brain Communication, Kochi University of Technology, Kochi, 782-8502, Japan
[c] Graduate School of Informatics, Nagoya University, Nagoya, 464-8601, Japan
[d] Center for Information and Neural Networks, National Institute of Information and Communications Technology, Osaka, 565-0871, Japan

ARTICLE INFO

Keywords:
Ventromedial prefrontal cortex
Amygdala
Caudate nucleus
Physiological arousal
Reward
Dynamic causal modeling
Post-hoc Bayesian model selection

ABSTRACT

When preparing for a challenging task, potential rewards can cause physiological arousal that may impair performance. In this case, it is important to control reward-driven arousal while preparing for task execution. We recently examined neural representations of physiological arousal and potential reward magnitude during preparation, and found that performance failure was explained by relatively increased reward representation in the left caudate nucleus and arousal representation in the right amygdala (Watanabe, et al., 2019). Here we examine how prefrontal cortex influences the amygdala and caudate to control reward-driven arousal. Ventromedial prefrontal cortex (VMPFC) exhibited activity that was negatively correlated with trial-wise physiological arousal change, which identified this region as a potential modulator of amygdala and caudate. Next we tested the VMPFC - amygdala - caudate effective network using dynamic causal modeling (Friston et al., 2003). Post-hoc Bayesian model selection (Friston and Penny, 2011) identified a model that best fit data, in which amygdala activation was suppressively controlled by the VMPFC only in success trials. Furthermore, fixed connectivity strength from VMPFC to amygdala explained individual task performance. These findings highlight the role of effective connectivity from VMPFC to amygdala in order to control arousal during preparation for successful performance.

1. Introduction

People naturally tend to feel nervous before performing an important task, such as a solo musical act in front of an audience. The effectiveness of an individual's performance can be impacted by the magnitude of the potential reward (e.g. recognition of the audience) and the elicited reward-driven arousal (i.e.nervousness about being well-received by the audience). In such situations, controlling reward-driven arousal prior to task-execution is critical for maximizing potential rewards (Yerkes and Dodson, 1908; Ariely et al., 2009). In a recent study (Watanabe et al., 2019), we investigated how neural representations of arousal and potential reward while preparing to perform a task lead to failure or success. The results highlighted how failures in performance were explained by relatively increased reward magnitude representation in the left caudate nucleus and physiological arousal representation in the right amygdala during task preparation. A remaining question, however, is how successful task performance is achieved? In this study, we examine network dynamics involving reward-related caudate activity, arousal-related amygdala activity, and prefrontal cortex. Particularly, we examine how prefrontal cortex may interact with caudate and amygdala during task preparation in order to regulate reward-driven arousal and perform the task successfully.

Previous studies highlight the role of several subregions of the prefrontal cortex for the control of reward and arousal information. For example, Pessoa (2009) proposed that anterior cingulate cortex (ACC), dorsolateral PFC (DLPFC), and inferior frontal gyrus (IFG) are important for the integration of emotional and motivational information. Salzman and Fusi (2010) suggested that orbitofrontal cortex (OFC) and ACC represent the interaction between emotion and cognition. Ochsner and Gross (2008) also highlighted the contribution of lateral PFC (LPFC), ACC

* Corresponding author. Research Center for Brain Communication, Kochi University of Technology, 185, Miyanokuchi, Tosayamada, Kami, Kochi, 782-8502, Japan.
** Corresponding author. Department of Psychology, Rutgers University, 101 Warren Street, Newark, NJ, 07102, USA.
E-mail addresses: noriyawtnb@gmail.com (N. Watanabe), delgado@psychology.rutgers.edu (M.R. Delgado).

https://doi.org/10.1016/j.neuroimage.2019.116136
Received 16 July 2019; Received in revised form 23 August 2019; Accepted 27 August 2019
Available online 27 August 2019

and medial PFC (MPFC) during emotion regulation. Although all these regions can have potential roles as modulators, we highlight the contributions of ventromedial prefrontal cortex (VMPFC) specifically to the regulation of physiological arousal and reward valuation (Delgado et al., 2016), processes that are critical to controlling reward-driven arousal for successful task performance.

First, VMPFC contributes to modulation of the autonomic arousal system. Human VMPFC lesions disrupt anticipation-related physiological arousal measured by skin conductance response (Damasio et al., 1990). Functional magnetic resonance imaging (fMRI) research also demonstrates that VMPFC is inversely correlated with physiological arousal level (Fan et al., 2012; Nagai et al., 2004) and VMPFC may suppressively modulate arousal change (Zhang et al., 2014). Therefore, compared to other sub-regions in PFC, VMPFC activity has been more consistently associated with autonomic changes.

Second, with respect to reward valuation, the communication between VMPFC and striatum plays a role in representing expected value (i.e. potential reward magnitude that an individual expects to earn). VMPFC lesions disrupt both flexible updating of value (Tsuchida et al., 2010; Rudebeck et al., 2013; Schneider and Koenigs, 2017) and maintenance of a choice over successive decisions based on the value (Henri-Bhargava et al., 2012; Noonan et al., 2012). VMPFC also directly projects to the ventral striatum including the ventromedial area of the caudate nucleus (Sesack et al., 1989; Gabbott et al., 2005; Choi et al., 2017; Lehericy et al., 2004) and it may flexibly control a value signal in the striatum according to the current goals (Ferenczi et al., 2016; Ghazizadeh et al., 2012). In both cases, however, it is not clear how the VMPFC regulates the amygdala and striatum to control physiological arousal and/or value signal during task-preparation and how these network dynamics contribute to actual performance.

In the current study, we conducted dynamic causal modeling (DCM: Friston et al., 2003) analysis, which makes it possible to infer the functional causal networks of given multiple seed regions. We used this approach to investigate the contribution of the prefrontal cortex to control reward-related caudate and arousal-related amygdala activity. First we identified a potential prefrontal subregion in VMPFC that was involved in the control of physiological arousal from a data set reported in Watanabe et al. (2019). Then we tested how functional coupling of the VMPFC and amygdala and/or caudate would contribute to suppressive control of physiological arousal and/or reward value signal during preparation to perform a stop-watch task for a monetary reward stake that varied trial-to-trial. We tested these hypotheses with DCM with Post-hoc Bayesian Model Selection (Friston and Penny, 2011; Rosa et al., 2012) and described a model of VMPFC-amygdala suppression for control of physiological arousal during preparation to execute a task for monetary reward.

2. Materials and methods

2.1. Participants and task

We applied dynamic causal modeling to the data set published in Watanabe et al. (2019). Participants were from the Rutgers University community with no history of psychiatric or neurological disorders. All participants gave informed consent and procedures were conducted according to the principles in the Declaration of Helsinki and were approved by the Rutgers University Institutional Review Board. The number of participants was 22 (14 female, mean age 21.3, standard deviation (SD) = 2.4, range 18–27 years old). We evaluated trial-by-trial physiological arousal and performance by pupillometry and a stop-watch task (SW task: Fig. 1A). In this task, participants were presented with a "GO" signal which indicated they had 5 s to press a button. Their accuracy in this "stop-watch" determined whether they would earn a reward (success) or not (failure). The value of the reward was predetermined prior to the onset of the trial and presented 5.5 s before the GO signal, during the preparatory phase ("SET" signal). Participants were presented with the reward stake (changing from $0.50 to $40.00 for each trial) and we measured arousal induced by the presentation of the reward, during task preparation, before they could execute the stop-watch task. The pupil amplitude for each trial was collected at this preparatory SET phase and all data were *z*-normalized by each session. Participants were engaged in 80 trials with three sessions in the MRI scanner after another training without monetary incentives. All behavioral data and pupil data analysis as reported previously (Watanabe et al., 2019). This SW task was 'challenging' in the sense that the success rate was low (Mean ± SD = 39.9 ± 10.1%) and perceived as subjectively difficult (ratings of difficulty were greater than zero (neutral): one sample $t(21) = 4.915$, $p = 0.038$).

2.2. Equipment

Brain images were collected by a 3 T Magnetom TRIO scanner with a 12-channel head coil (Siemens, Erlangen, Germany). For pupillometry, a SR search EyeLink 1000 Plus system was used. We tracked pupil diameter from the right eye with 500 Hz sampling rate with the centroid mode to reduce the noise in the pupil data. For stimulus presentation and data analysis, we used MATLAB R2015a (Mathworks, Natick, MA, USA) with Psychtoolbox 3.0.12 (Brainard, 1997; Kleiner et al., 2007). We used MATLAB R2015a with Statistical Parametric Mapping 12 (SPM12) revision 6685 for evaluation of functional localization and Dynamic Causal Modeling 12 (DCM12) for evaluation of effective connectivity analysis (Friston et al., 1995; Wellcome Department of Imaging Neuroscience, London, UK).

2.3. Mean pupil amplitude

We tracked eye-pupil dynamics during preparation to perform the task. Pupil amplitude as well as skin conductance responses are widely used for detection of trial-wise physiological arousal response (Bradshaw, 1967; Partala and Surakka, 2003; Bradley et al., 2008; O'Reilly et al., 2013; Preuschoff et al., 2011). The pupil amplitude data were preprocessed and analyzed using a custom script that utilized MATLAB signal processing functions to remove the artifacts in the time series (see Watanabe et al., 2019 for details). The pupil regressor was the mean pupil size during the preparatory phase (5.5s) to represent trial-wise physiological arousal change.

2.4. Data acquisition and analysis of fMRI data

Data acquisition is reported in Watanabe et al. (2019). Preprocessing consisted of standard steps for each participant's functional data: slice timing correction, image realignment to the mean volume, spatial normalization to the Montréal Neurological Institute (MNI) standard (resampled at 2 mm^3), and spatial smoothing (8-mm Gaussian kernel). Prior to dynamic causal modeling, we estimated a general linear model to identify regions that potentially exercise control over physiological arousal and/or reward expectation. This model included trial-wise pupil amplitude, reward magnitude and the interaction (pupil x reward) as parametric modulators at the preparatory SET phase. The regions of interest were identified by a negative relation to the pupil or reward parametric regressor, suggesting control over arousal or reward representation. This definition is similar to Zhang et al. (2014), Fan et al. (2012), and Nagai et al. (2004). Additionally, the regressor set included onset of the PRESS and FEEDBACK phase with a parametric modulator representing feedback reward size. Regressors describing head motion (24 total) and eye movements (4 total) were included as regressors of no interest.

2.5. Identification of a region involved in control of arousal and incentive representations

To identify regions that potentially control arousal or reward value

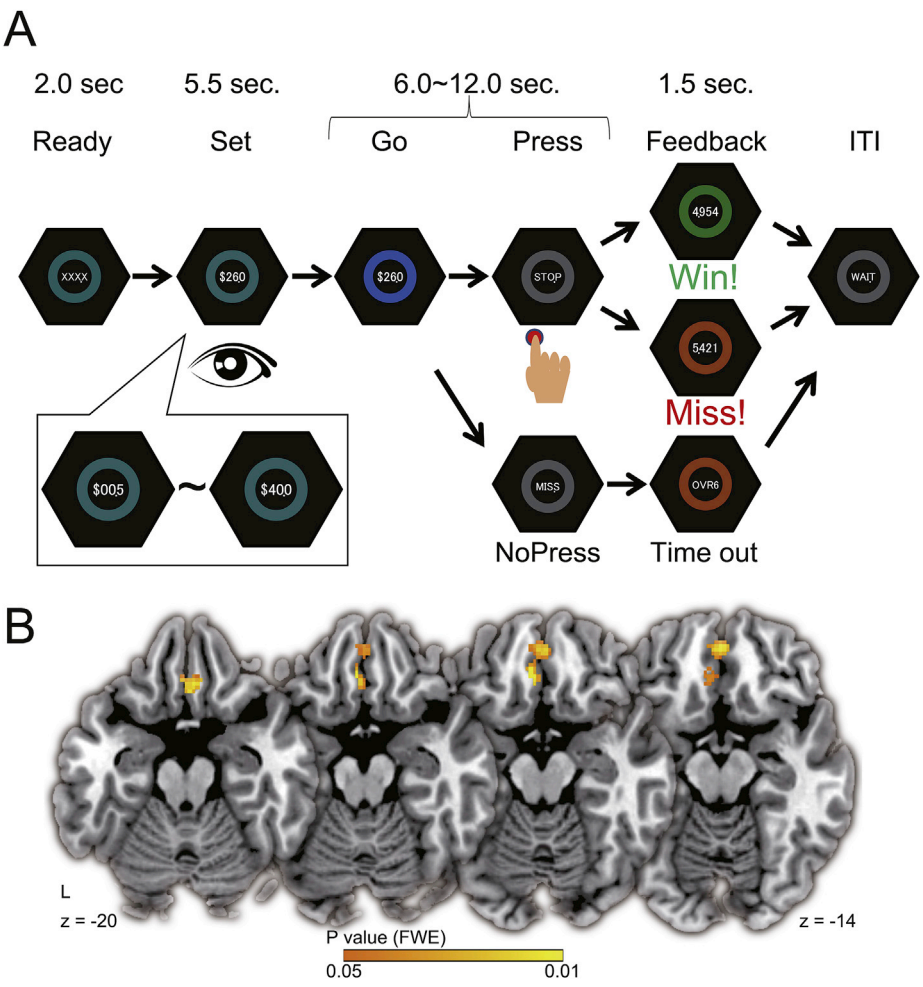

Fig. 1. Stop-watch task procedure (adapted from Watanabe et al., 2019) and brain activation negatively correlated with mean pupil amplitude during preparatory SET phase. A) On each trial, participants first prepared for task execution while knowing the reward amount at stake, then executed the stop-watch task. At READY phase, a lime-colored ring and 4 letters "XXXX" indicate the start of a trial. At the SET preparatory phase (red frame), a monetary offer was presented (e.g. $26.0) and pupil response was collected. The magnitudes of reward offer were changed every trial and varied between $0.50 and $40.00 (shown in inset). Participants counted 5 s in their heads from the GO signal (blue ring) and pressed the button to stop the watch (PRESS). Response time was shown at the FEEDBACK phase resulting in monetary reward for a press within an allowable margin around 5.0 s (Success), or no reward for presses outside the margin (Failure) and trials without a press within 6 s (Time out). Analysis focused on neural signal changes related to the preparatory SET period. B) Brain activity negatively correlated with pupil amplitude across all trials. Presented threshold is $p < 0.05$, FWE correction and masked by the anatomically defined prefrontal cortex.

representations in the brain, we investigated activation in prefrontal cortex (PFC) which negatively correlated with pupil or reward magnitudes. Although we were especially interested in VMPFC (Zhang et al., 2014; Nagai et al., 2004), we did not limit the search volume within PFC because several subregions, including DLPFC, PFC, IFG, ACC, and MPFC, have been potentially associated with 'control' and 'regulation' of arousal and incentive representations in prior experiments (Pessoa, 2009; Salzman and Fusi, 2010; Ochsner and Gross, 2008; Delgado et al., 2008). Results were corrected for multiple comparisons within the search volume, which encompassed all PFC regions.

2.6. Additional preprocessing for reduction of motion related distortion

Prior to dynamic causal modeling analysis, we applied additional motion reduction methods as brain connectivity results can be severely distorted by head motion (Power et al., 2012, 2015). These additional preprocessing steps were carried out using tools from FSL (FMRIB Software Library version 5.0.4; http://www.fmrib.ox.ac.uk/fsl). First, we identified motion spikes according to two metrics: 1) root-mean-square (RMS) intensity difference of each volume relative to a reference volume; and 2) frame-wise displacements computed as the mean RMS change in rotation/translation parameters relative to the reference volume. For each metric, we used a boxplot threshold (i.e. 75th percentile plus 1.5 times the interquartile range) applied to the metric values within one run to classify volumes as spikes. This procedure classified an average of 9.9% of volumes as spikes (range: 5.6–18.3%). All spikes were then removed via regression, as well as variance described by extended motion parameters (i.e. squares, temporal differences, and squared temporal differences) (Power et al., 2015; Satterthwaite et al., 2013).

2.7. Dynamic causal modeling (DCM)

After additional controls to help mitigate the influence of head motion on connectivity results, we created a new design matrix for DCM (Friston et al., 2003). The main goal of this analysis was to clarify how one modulatory factor, performance (i.e. success or failure), may influence network connections between caudate nucleus, amygdala and PFC. To accomplish this goal, we examined a full set of possible models of where the driving factor and modulatory factor (described below) could influence the network.

Regressor of driving factor: The driving factor represents extrinsic influences on neuronal activity, evoked by the stimulus. In the present study, the onset of the preparatory SET phase (both success and failure trials) drove the system, and this driving factor could influence any combination of nodes in the network. The mean pupil amplitude, reward magnitude and interaction of pupil and reward were also included in the model as effects of interest.

Regressor of modulatory factor: The modulatory factor represents a context-dependent change in connectivity (i.e. a difference in the network depending on whether the preparation period resulted in success or failure on each trial). In our model, we were interested in changes in the network for successful trials because failure trials were linked to lack of control over reward-driven arousal (Watanabe et al., 2019). Thus, we used the onset of the preparatory set phase of success trials as the modulatory factor. In this way, the modulatory effect represented a change in the network during preparation on successful trials, in

reference to all (i.e. both success and failure) trials.

Other regressors: the timing of PRESS, FEEDBACK phase and earned reward magnitude were included in the model as effects of non-interest.

2.7.1. Selection of regions for the network

Three regions of the network were defined based on Watanabe et al. (2019) and the current analysis. The first region was the right amygdala (group level peak coordinate: x = 22, y = 6, Z = −16) which was identified as relatively higher pupil-related representation in failure compared to success trials. This amygdala activity was the only cluster which survived FWE correction ($p < 0.05$) in this contrast. The second region was the VMPFC (x = −6, y = 34, z = −16) which was identified as the only cluster within PFC that negatively correlated with trial-wise pupil change (see the Results section in this article). The third region was the left caudate nucleus (x = −6, y = 18, z = 0), which showed relatively greater representation of reward magnitude in failure compared to success trials. This caudate activity was the only cluster which survived FWE correction ($p < 0.05$) in this contrast.

We chose these three regions to test whether the VMPFC exerted influence over arousal-related amygdala and/or reward-related caudate activity during the preparatory phase in success compared with all trials by DCM. Although reward magnitude did not directly influence performance, we included the reward-related caudate region in our DCM because (a) reward magnitude indirectly related to performance through its influence on arousal change (which did relate to performance) and (b) reward-related caudate activation was related to performance (greater in failure compared to success trials).

BOLD time-series of volumes of interest (VOI) in the three regions were extracted from 4 mm radius spheres centered on the individual peak voxel within a regional mask. Each regional mask was defined by the intersection of 1) anatomically defined, amygdala, prefrontal cortex or caudate nucleus from the automated anatomical labeling (AAL) template (Tzourio-Mazoyer et al., 2002) and 2) identified group level clusters from right amygdala, left caudate, and VMPFC. An F contrast constructed by driving inputs (d) and modulatory input (m) was used to extract time-series data.

2.7.2. Model constraints

Although the DCM assesses effective connectivity based on BOLD signal and not direct observation of actual neural activity, it is recommended to use anatomical information as a prior to improve the model likelihoods (Stephan et al., 2010). The usefulness of structural constraints for model fitting has also been statistically evaluated and confirmed (Stephan et al., 2009; Sokolov et al., 2019). For these reasons, we added network constraints based on well-established anatomical evidence to define the full model for post-hoc Bayesian model selection in the current analysis.

Anatomical connections exist from VMPFC to the amygdala (Amaral and Insausti, 1992; Carmichael and Price, 1995) and from VMPFC to the ventromedial area of caudate (Sesack et al., 1989; Gabbott et al., 2005; Choi et al., 2017; Lehericy et al., 2004). Amygdala also has dense projections to VMPFC (Amaral and Price, 1984; Barbas and De Olmos, 1990) and to caudate (Fudge et al., 2002; Russchen et al., 1985). However, less is known about direct anatomical projection from rostral caudate to amygdala (Freese and Amaral, 2009), or from rostral caudate to VMPFC (Haber and Knutson, 2010). Therefore, we removed connections from caudate to amygdala and from caudate to VMPFC from the full model in the present study. We did not impose any constraints on driving nor modulatory inputs as there are several possible variations of starting points and modulations in the network.

2.7.3. Model selection and parameter evaluation

The model selection step in DCM is often conducted with specific multiple hypotheses about possible structures of the network and the restricted set of models is compared by its fit to the data. However, there is a possibility with this approach that the true optimal model is not captured or there is an intractable number of models to evaluate (i.e. combinatorial explosion of models; Friston and Penny, 2011; Lohmann et al., 2012). Instead, we used Post-hoc Bayesian Model Selection, a Bayesian model reduction approach that searches large model spaces in an unbiased way (Friston and Penny, 2011; Rosa et al., 2012). This procedure estimates an "optimized model" from the "full model" which contains all possible combinations of free parameters by reducing parameters based on evidence (marginal likelihood).

After the adoption of the constraints shown above, the full model contained 2048 combinations of three possible driving inputs (2^3 combinations), four fixed connections (2^4 combinations) and four modulatory inputs (2^4 combinations). We then used post-hoc Bayesian model selection to find the optimal network from the 2048 possible combinations in the full model. This model reduction step operates at the group level by pooling the evidence for each individual model (i.e. each of 2048 possible networks). The best model has the highest evidence as determined by Bayes factor. Ratio of evidence for the best versus second best model was used to evaluate confidence for the optimized model (Penny et al., 2004). The parameter estimates (E) and model posterior probability (P) are calculated by group level Bayesian parameter average (BPA) under the selected model.

2.7.4. Robust regression analysis

We next examined whether individual connection strengths in the optimal network, that were estimated for each participant, can explain individual differences in performance. The question is whether individual differences in effective connectivity at specific locations in the network explain individual performance. Individual parameter estimates of fixed connections (baseline connectivity) and modulatory inputs (change in connection strength for success trials) were extracted for each participant. We used a robust regression analysis with bi-square weights to examine relationships between these parameters and individual performance (mean timing performance score). This method ensures that the results are not overly influenced by outlier values and is recommended to use with small sample sizes in neuroimaging individual differences analyses (Poldrack, 2012).

Individual mean timing performance score was calculated by the following equation,

$$Timing\ \ Performance\ Score = 1 - (|5.00 - RT|/5.00)$$

This individual performance score is 1.0 when the Response Time (*RT*) is exactly 5 s and is lower the more *RT* deviates from 5 s. A trial was excluded from analysis when *RT* was less than 3 s (performance scores ranged from 0.6 to 1.0). One trial was excluded from 6 participants, two trials from 3 participants and three trials from 1 participant (mean ± SD exclusion = 0.681 ± 0.873 trials). Individual parameter estimates *E* were extracted from 'DCM_opt_XXX.m', which is the individual level Bayesian parameter average (BPA) under the optimized model after model selection. This measure represents the connection strength for each participant for each connection under the optimal model. The *E* of seven fixed connections and four modulatory inputs were used for the comparison with the task performance. The correlation between an fixed connection and performance indicates that the strength of the connection during the preparatory phase across all trials explains individual performance. Correlation between a modulatory input and performance indicates that change in the connection during success trials explains individual performance. Family-wise error (FWE) correction for multiple comparisons was applied in the regression analysis (11 comparisons).

Group level data for this article are publicly available at "https://osf.io/2y786/?view_only=fb9d8296b07a4ffc997d2d4bee92d1c9" in a page at Open Science Framework (OSF: https://osf.io/).

3. Results

In the previous report (Watanabe et al., 2019), we examined how

potential reward and its influence on arousal, measured by pupil dynamics, are represented in the brain while participants were preparing to perform a stop-watch task. Trials resulting in performance failure were characterized by increased pupil dilation as a function of increasing reward magnitude during preparation. Such failure trials were associated with activation of the right amygdala representing pupil dilation, and the left caudate nucleus representing reward magnitude. Whereas the previous report evaluated how arousal during preparation interfered with performance, here we investigated how prefrontal cortex controlled the arousal-related amygdala and reward-related caudate activation to facilitate better performance via dynamic interactions.

3.1. BOLD signal in VMPFC is inversely correlated with mean pupil amplitude

To find potential modulators of amygdala and caudate activity, we first investigated BOLD signals in PFC that were negatively correlated with trial-wise physiological arousal or with trial-wise reward magnitude at the preparatory SET phase. The search was performed across the entire PFC and a cluster in the VMPFC was uniquely identified (Table 1). Specifically, we observed an inverse correlation between VMPFC and arousal level across all trials (Fig. 1B; peak voxel: $x = -6$, $y = 34$, $z = -16$, $t = 6.06$, $p = 0.001$ FWE corrected). On the other hand, we did not identify any significant activity which was negatively correlated with trial-wise reward magnitude in PFC, even at a more liberal threshold ($p < 0.001$, uncorrected).

The negative representation of trial-wise arousal in VMPFC suggests a potential relationship with arousal-related amygdala activity. It leads to the idea that functional modulation from the VMPFC to the amygdala may potentially change on success trials as a function of some form of cortical control. Together with previous evidence of VMPFC modulation of value signals in the striatum (Ferenczi et al., 2016; Ghazizadeh et al., 2012), we next investigated the effective connectivity among VMPFC, amygdala and caudate nucleus using DCM in order to test whether this network would differ between trials resulting in success and failure when preparing to perform. More specifically, we tested whether this VMPFC activity suppressed the amygdala and/or caudate activity to facilitate successful performance.

3.2. VMPFC and amygdala interaction changed in success trials

Post-hoc Bayesian model optimization from the full model (Fig. 2A) found one winning model (Fig. 2B) from 2048 possible combinations. This model has the highest posterior probability (87.0%) and the ratio of this best and the second best model probability (Penny et al., 2004) was $87.0/5.7 = 15.26$, indicating strong evidence for the chosen model being the best explanation. In this optimized model, two possible driving inputs (VMPFC and caudate) and two possible modulatory inputs (from VMPFC to caudate, and from amygdala to caudate) were evaluated as unnecessary parameters by the optimization. Under the optimized model, the amygdala was evaluated as the ideal driving point of this network, and connection change related to success trials (i.e. the modulatory effect) was limited to the connections between VMPFC and amygdala (i.e. VMPFC to amygdala, and amygdala to VMPFC). Bayesian parameter average (E) under the selected model (Fig. 2B) showed that effective connectivity from VMPFC to amygdala was associated with a positive connection in general ($E = 0.031$) but, in success trials, this connection changed to a negative value ($0.031–0.113 = -0.082$). This means that the effect from VMPFC to amygdala was changed from enhancement to suppression on success trials, whereas the positive connection from amygdala to VMPFC was increased in success trials ($0.010 + 0.143 = 0.153$).

To better understand this result, we also investigated the beta estimates of each seed and their correlations (Supplemental Fig. S1). This analysis revealed that the correlation between the individual beta estimates from VMPFC and amygdala were significantly positive in success trials ($r = 0.588$, $p = 0.024$ Bonferroni correction) and also that the correlation in failure trials showed similar positive tendency ($r = 0.453$, $p = 0.205$ Bonferroni correction), though the correlation was not statistically significant in failure trials. This group level relationship contributed the overall positive effective connectivity between VMPFC and amygdala in the DCM results.

In addition to the DCM with three seeds, we evaluated another model with eight seeds which included other regions identified by the same negative relation to pupil size that was seen in VMPFC (see Supplemental Methods and Fig. S2 for detail). The additional model included superior occipital gyrus, postcentral gyrus, superior temporal gyrus, and superior parietal cortex in addition to the original three regions. This eight seed DCM was consistent with the original three seed model in the sense that the amygdala was suppressively modulated by VMPFC (Supplemental Fig. S3). Additional results and discussion are included in Supplemental Results.

Table 1
Negative correlation with mean pupil size ($p < 0.05$ FWE, cluster size ≥ 20).

Area	L/R	x	y	z	k	T	peak P (FWE)
Superior occipital gyrus	R	26	−78	30	7999	10.23	<0.001
Postcentral gyrus	R	48	−26	58	2576	7.40	<0.001
Precentral gyrus	L	−34	−24	56	1787	7.33	<0.001
Superior temporal gyrus	L	−58	−16	4	346	7.08	<0.001
Superior temporal gyrus	R	62	−10	2	739	6.74	0.001
Precentral gyrus	R	62	10	24	50	6.30	0.002
Supra marginal gyrus	R	64	−16	28	76	6.10	0.004
Ventromedial prefrontal cortex	**R**	**−6**	**34**	**−16**	**153**	**6.06**	**0.004**
Superior parietal cortex	R	16	−54	64	153	6.03	0.004
Superior parietal cortex	L	−30	−56	56	22	5.53	0.018

3.3. Strength of VMPFC to amygdala connection explained individual performance

We further investigated the relationship between connectivity strength from VMPFC to amygdala and individual performance or subjective ratings about difficulty, effort, pressure and fatigue levels. Robust regression analyses showed that the fixed connection strength from VMPFC to amygdala explained 57.5% of variance in performance (Fig. 2C: $t(20) = 5.157$, $R^2 = 0.575$, $p = 0.0005$ Bonferroni correction). The other six fixed connections did not explain performance ($t(20) < 1.442$, $R^2 \leq 0.094$, $p \geq 0.165$ uncorrected). We also tested the relationship between modulatory input and individual performance, but there was no significant correlation between any modulatory inputs and performance. Finally, we did not observe any significant relation between effective connectivity and subjective ratings.

4. Discussion

How do our brains control reward-driven arousal during task preparation in order to improve performance? To investigate mechanisms involved in controlling physiological arousal and reward expectation, we re-analyzed fMRI brain data in Watanabe et al. (2019) with dynamic causal modeling (DCM) and focused on the connectivity of three ROIs during preparation to perform a stop-watch task for monetary incentives. First, we identified a ROI in the VMPFC where activation was inversely correlated with trial-wise pupil amplitude during the preparatory period preceding trial performance. This inverse relationship is consistent with previous reports of VMPFC associations to arousal measured by skin conductance level (Nagai et al., 2004; Fan et al., 2012; Zhang et al.,

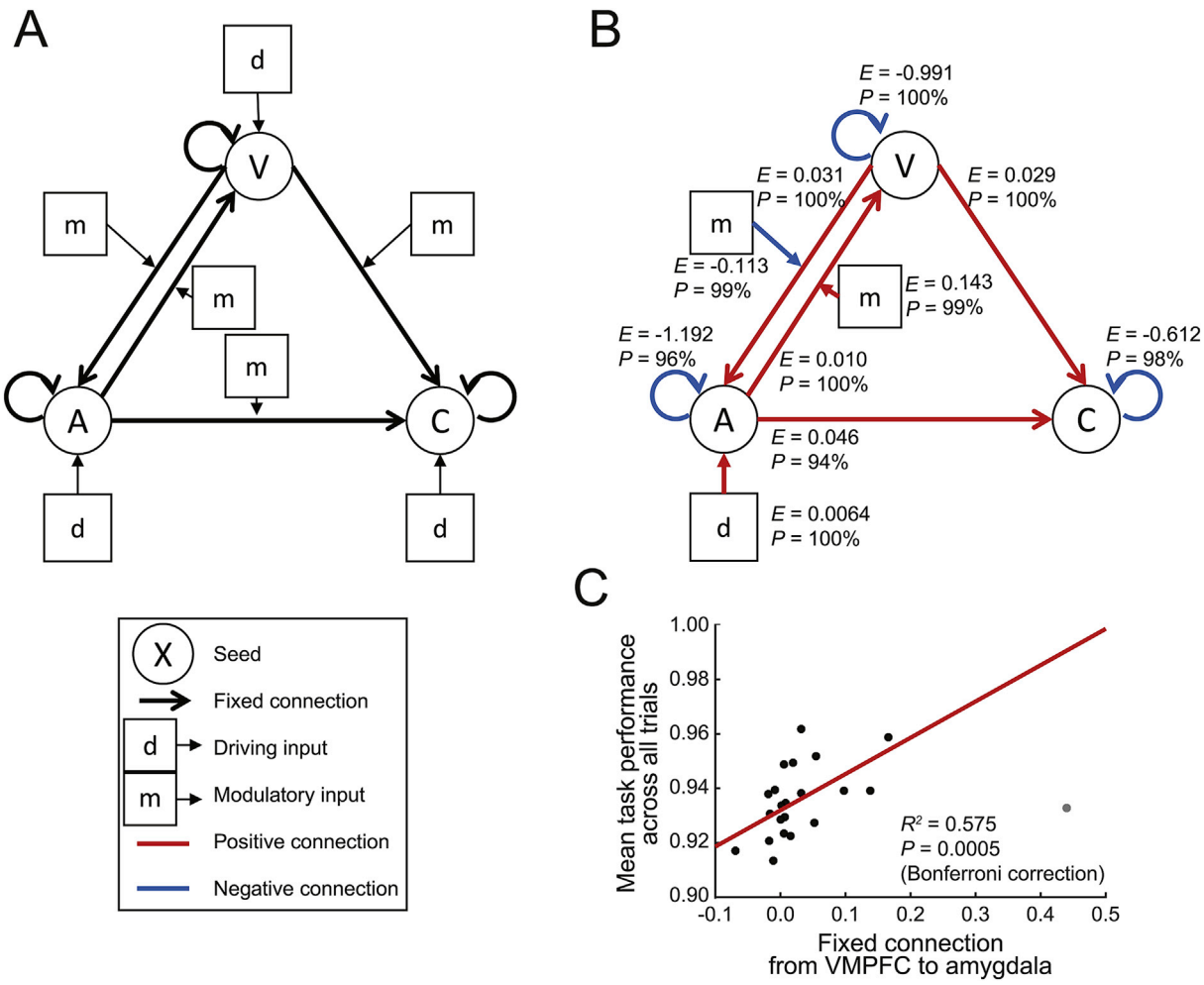

Fig. 2. Results of model optimization, and estimated parameter – performance positive relationship. A) Full model and B) optimized model by post-hoc Bayesian model selection. Each value represents Bayesian parameter average (*E*) and model posterior probability (*P*). A, V, C indicate amygdala, VMPFC and caudate nucleus respectively. C) The strength of the fixed connection from VMPFC to amygdala explained individual mean performance across success and failure trials. Red line indicates robust regression line.

2014). Then we tested whether this activation was consistent with the hypothesis that the VMPFC modulated arousal-related amygdala and/or value-related caudate activity. DCM with Post-hoc Bayesian model selection revealed that VMPFC modulated both amygdala and caudate through fixed connections, but only VMPFC and amygdala interaction was changed on trials resulting in successful performance, and this interaction was bi-directional. In particular, the effective connectivity from VMPFC to amygdala changed from positive to negative modulation in success trials. Furthermore, the fixed connection strength from VMPFC to amygdala explained individual differences in task performance. These results highlight how reward-driven arousal prior to task execution is suppressed by VMPFC which can consequentially impact successful performance.

4.1. VMPFC controls amygdala activation to facilitate successful performance

The current results describe a neural mechanism for controlling physiological arousal during preparation that affects subsequent behavioral performance. Although prior research has suggested that VMPFC may contribute to task performance, there has been no direct evidence how the VMPFC modulates other brain regions and changes behavioral performance (Nagai et al., 2004; Zhang et al., 2014). We examined this important question with DCM analysis, and findings show that VMPFC suppressed arousal-related amygdala activation specifically in success trials. These dynamics are interesting because VMPFC and amygdala fixed connectivity (i.e. across all trials) was positive in both directions, but VMPFC suppressed the amygdala activation only in success trials. This observed suppressive regulation of the amygdala by VMPFC is consistent with negative relationships between VMPFC and amygdala in emotion regulation (Urry et al., 2006; van Reekum et al., 2007) and fear extinction (Phelps et al., 2004; Delgado et al., 2008) observed with neuroimaging, as well as disinhibited amygdala response observed in VMPFC lesion patients (Motzkin et al., 2015).

An important question is how the VMPFC, which outputs glutamate projections to amygdala, impacts modulation of amygdala from enhancement to suppression in success trials. One potential explanation is in GABAergic neurons of the intercalated cell clusters (ITC) in amygdala (Ehrlich et al., 2009; Johansen et al., 2011). VMPFC has projections both into glutamatergic and GABAergic neurons at subnuclei in amygdala and this system is thought to contribute to emotion regulation and fear extinction (Hartley and Phelps, 2010; Kim et al., 2011a,b). Our results suggested that a system for performance optimization overlaps with the previously described system for fear extinction and emotion regulation. However, MRI is limited in spatial and temporal resolution needed to investigate specific subnuclei in amygdala, and additional non-human research is required to directly investigate it with a challenging task like the SW task.

As our current DCM design compared success trials in reference to all trials, it is difficult to evaluate how connectivity changed specifically in

failure trials. However, the group level correlation analysis across three seeds (Supplemental Fig. S1) suggested additional details between VMPFC and amygdala. The correlation between these two seeds was significant only in success trials but not in failure trials. This observation may relate to VMPFC – amygdala synchronization during the task and the synchronization level was decreased in the failure trials.

Furthermore, individual difference analysis showed that the strength of the fixed connection from VMPFC to amygdala positively related to better task performance. A previous study suggested that greater VMPFC – amygdala resting state functional connectivity is correlated with successful emotion regulation, such as fear extinction (Feng et al., 2016). Meanwhile, decreased functional connectivity between VMPFC – amygdala is associated with high anxiety, which is characterized by difficulty controlling arousal (Kim et al., 2011a,b; Hahn et al., 2011). Therefore, the positive relationship between the connectivity and performance in the current study suggests that the strength of effective connectivity from VMPFC to amygdala is important for controlling reward-driven arousal to perform the task.

In contrast to the modulation between VMPFC-amygdala by task performance, we did not observe any modulation of the interaction between VMPFC and caudate. This means the information flow from VMPFC to caudate was not changed by success and failure trials. One potential reason of this unexpected result is that the trial-wise subjective motivation for winning the game was not different between success and failure trials. In our study, individual performance was not simply affected by the magnitude of reward presented (see behavioral results in Watanabe et al., 2019), but performance was affected by trial-wise physiological arousal level. A possible interpretation is that, under the demands of this task, control of physiological arousal by VMPFC-amygdala interaction may be more important than the control of a value signal by VMPFC-caudate interaction.

4.2. Limitations

Although we described a VMPFC – amygdala – caudate network that contributes to control of physiological arousal, the analysis included some limitations. First, DCM requires specific seed regions prior to model evaluation. Although the three regions that were examined (see Model constraints in Methods) as well as the expanded eight regions (see Supplemental Methods and Fig. S2) have strong anatomical connections, we could not exclude potential contributions of other regions. In particular, the current analysis did not include locus coeruleus, which is a key node for physiological arousal, or dopaminergic nuclei (i.e. ventral tegmental area, substantia nigra) - key nodes for value estimation. Signal in these regions was not identified because our fMRI parameters were not optimized to detect BOLD signal in the brainstem. We also did not include right inferior frontal cortex as a seed which was identified by the interaction of pupil size and reward magnitude in the previous report (Watanabe et al., 2019) to avoid model complexity.

Second, the current DCM results also showed that the connection from VMPFC to caudate was not modulated by performance success. Previous studies suggest that VMPFC has a role in optimizing goal-directed behavior by regulating a value signal in the caudate (Pujara et al., 2016; Ferenczi et al., 2016; Ghazizadeh et al., 2012), but our findings do not allow for inferences about a similar role for VMPFC in preparation to perform the SW-task. One possible reason for this inconsistency is that, because we defined the VMPFC region based on the pupil amplitude related regressor, the seed selection was better suited to identify the VMPFC – amygdala connection rather than a VMPFC – caudate connection. We did not identify any prefrontal activation negatively related to reward value, which might better identify prefrontal – caudate connections with implications for successful performance.

5. Conclusion

We investigated functional brain connections for succeeding in a challenging task while experiencing reward-driven arousal during task preparation. We identified suppressive modulation of amygdala by VMPFC, which related to successful task performance. This interaction can be a target for enhancing human task performance under highly pressured situations. Future studies could examine potential for manipulation of connectivity from VMPFC to amygdala by neurofeedback to enhance task performance.

Additionally, the findings potentially inform new treatments for patients with anxiety disorder who have difficulties regulating their emotion flexibly and are faced with severe performance deterioration from anxiety (Amstadter, 2008). Brain dynamics in anxiety disorder are characterized by hyper activity of amygdala and failure to recruit VMPFC (Milad et al., 2006; Quirk and Gehlert, 2003) and by reduced positive resting-state functional connectivity between VMPFC – amygdala (Kim et al., 2011a,b; Hahn et al., 2011). Examining the preparatory phase before task performance may provide an ideal period of investigation to measure individual differences in VMPFC and amygdala functional connectivity which may be associated with clinical symptomology.

Conflicts of interest

None declared.

Acknowledgement

We are grateful to Dr. Masahiko Haruno in NICT, Dr. Hideki Ohira in Nagoya University, and Dr. Masaki Takeda in Kochi University of Technology for helpful discussion. We would like to thank Dr. Takanori Kochiyama in Advanced Telecommunications Research Institute for technical advice of DCM analysis. We also thank members of the Delgado Lab for constructive advice, and Mr. Gregg Ferencz and Dr. Stephen Hanson for technical support of simultaneous data collection of eye-tracking and fMRI. This study was supported by funding from the National Institutes of Health to M.R.D. (DA027764), Grant-in-Aid for Young Scientists (B) (25780454 and 16K17358) from Japan Society for the Promotion of Science (JSPS), Grant-in-Aid for JSPS fellows (H26, Social Science, 2502), and JSPS Overseas Research Fellowships to N.W. in Japan, and a National Science Foundation SBE Postdoctoral Research Fellowship to J.P.B. (NSF SPRF 1305994).

Appendix A. Supplementary data

Supplementary data to this article can be found online at https://doi.org/10.1016/j.neuroimage.2019.116136.

References

Amaral, D.G., Insausti, R., 1992. Retrograde transport of D-[3H]-aspartate injected into the monkey amygdaloid complex. Exp. Brain Res. 88, 375–388.
Amaral, D.G., Price, J.L., 1984. Amygdalo-cortical projections in the monkey (Macaca fascicularis). J. Comp. Neurol. 230, 465–496.
Amstadter, A., 2008. Emotion regulation and anxiety disorders. J. Anxiety Disord. 22, 211–221.
Ariely, D., Gneezy, U., Loewenstein, G., Mazar, N., 2009. Large stakes and big mistakes. Rev. Econ. Stud. 76, 451–469.
Barbas, H., De Olmos, J., 1990. Projections from the amygdala to basoventral and mediodorsal prefrontal regions in the rhesus monkey. J. Comp. Neurol. 300, 549–571.
Bradley, M.M., Miccoli, L., Escrig, M.A., Lang, P.J., 2008. The pupil as a measure of emotional arousal and autonomic activation. Psychophysiology 45, 602–607.
Bradshaw, J., 1967. Pupil size as a measure of arousal during information processing. Nature 216, 515–516.
Brainard, D.H., 1997. The psychophysics toolbox. Spat. Vis. 10, 433–436.
Carmichael, S.T., Price, J.L., 1995. Limbic connections of the orbital and medial prefrontal cortex in macaque monkeys. J. Comp. Neurol. 363, 615–641.
Choi, E.Y., Ding, S.L., Haber, S.N., 2017. Combinatorial inputs to the ventral striatum from the temporal cortex, frontal cortex, and amygdala: implications for segmenting the striatum. eNeuro 4.
Damasio, A.R., Tranel, D., Damasio, H., 1990. Individuals with sociopathic behavior caused by frontal damage fail to respond autonomically to social stimuli. Behav. Brain Res. 41, 81–94.

Delgado, M.R., Beer, J.S., Fellows, L.K., Huettel, S.A., Platt, M.L., Quirk, G.J., Schiller, D., 2016. Viewpoints: dialogues on the functional role of the ventromedial prefrontal cortex. Nature Neuroscience 19, 1545–1552.
Delgado, M.R., Nearing, K.I., Ledoux, J.E., Phelps, E.A., 2008. Neural circuitry underlying the regulation of conditioned fear and its relation to extinction. Neuron 59, 829–838.
Ehrlich, I., Humeau, Y., Grenier, F., Ciocchi, S., Herry, C., Luthi, A., 2009. Amygdala inhibitory circuits and the control of fear memory. Neuron 62, 757–771.
Fan, J., Xu, P., Van Dam, N.T., Eilam-Stock, T., Gu, X., Luo, Y.J., Hof, P.R., 2012. Spontaneous brain activity relates to autonomic arousal. J. Neurosci. 32, 11176–11186.
Feng, P., Zheng, Y., Feng, T., 2016. Resting-state functional connectivity between amygdala and the ventromedial prefrontal cortex following fear reminder predicts fear extinction. Soc. Cogn. Affect. Neurosci. 11, 991–1001.
Ferenczi, E.A., Zalocusky, K.A., Liston, C., Grosenick, L., Warden, M.R., Amatya, D., Katovich, K., Mehta, H., Patenaude, B., Ramakrishnan, C., Kalanithi, P., Etkin, A., Knutson, B., Glover, G.H., Deisseroth, K., 2016. Prefrontal cortical regulation of brainwide circuit dynamics and reward-related behavior. Science 351 aac9698.
Freese, J., Amaral, D.G., 2009. Neuroanatomy of the primate amygdala. In: Whalen, P., Phelps, E.A. (Eds.), The Human Amygdala. Guilford, New York, pp. 3–42.
Friston, K., Penny, W., 2011. Post hoc Bayesian model selection. Neuroimage 56, 2089–2099.
Friston, K.J., Harrison, L., Penny, W., 2003. Dynamic causal modelling. Neuroimage 19, 1273–1302.
Friston, K.J., Holmes, A.P., Worsley, K.J., Poline, J.P., Frith, C.D., Frackowiak, R.S., 1995. Statistical parametric maps in functional imaging: a general linear approach. Hum. Brain Mapp. 2, 189–210.
Fudge, J.L., Kunishio, K., Walsh, P., Richard, C., Haber, S.N., 2002. Amygdaloid projections to ventromedial striatal subterritories in the primate. Neuroscience 110, 257–275.
Gabbott, P.L., Warner, T.A., Jays, P.R., Salway, P., Busby, S.J., 2005. Prefrontal cortex in the rat: projections to subcortical autonomic, motor, and limbic centers. J. Comp. Neurol. 492, 145–177.
Ghazizadeh, A., Ambroggi, F., Odean, N., Fields, H.L., 2012. Prefrontal cortex mediates extinction of responding by two distinct neural mechanisms in accumbens shell. J. Neurosci. 32, 726–737.
Haber, S.N., Knutson, B., 2010. The reward circuit: linking primate anatomy and human imaging. Neuropsychopharmacology 35, 4–26.
Hahn, A., Stein, P., Windischberger, C., Weissenbacher, A., Spindelegger, C., Moser, E., Kasper, S., Lanzenberger, R., 2011. Reduced resting-state functional connectivity between amygdala and orbitofrontal cortex in social anxiety disorder. Neuroimage 56, 881–889.
Hartley, C.A., Phelps, E.A., 2010. Changing fear: the neurocircuitry of emotion regulation. Neuropsychopharmacology 35, 136–146.
Henri-Bhargava, A., Simioni, A., Fellows, L.K., 2012. Ventromedial frontal lobe damage disrupts the accuracy, but not the speed, of value-based preference judgments. Neuropsychologia 50, 1536–1542.
Johansen, J.P., Cain, C.K., Ostroff, L.E., LeDoux, J.E., 2011. Molecular mechanisms of fear learning and memory. Cell 147, 509–524.
Kim, M.J., Gee, D.G., Loucks, R.A., Davis, F.C., Whalen, P.J., 2011a. Anxiety dissociates dorsal and ventral medial prefrontal cortex functional connectivity with the amygdala at rest. Cerebr. Cortex 21, 1667–1673.
Kim, M.J., Loucks, R.A., Palmer, A.L., Brown, A.C., Solomon, K.M., Marchante, A.N., Whalen, P.J., 2011b. The structural and functional connectivity of the amygdala: from normal emotion to pathological anxiety. Behav. Brain Res. 223, 403–410.
Kleiner, M., Brainard, D., Pelli, D., 2007. "What's New in Psychtoolbox-3?" Perception, vol 36 (ECVP Abstract Supplement).
Lehericy, S., Ducros, M., Van de Moortele, P.F., Francois, C., Thivard, L., Poupon, C., Swindale, N., Ugurbil, K., Kim, D.S., 2004. Diffusion tensor fiber tracking shows distinct corticostriatal circuits in humans. Ann. Neurol. 55, 522–529.
Lohmann, G., Erfurth, K., Muller, K., Turner, R., 2012. Critical comments on dynamic causal modelling. Neuroimage 59, 2322–2329.
Milad, M.R., Rauch, S.L., Pitman, R.K., Quirk, G.J., 2006. Fear extinction in rats: implications for human brain imaging and anxiety disorders. Biol. Psychol. 73, 61–71.
Motzkin, J.C., Philippi, C.L., Wolf, R.C., Baskaya, M.K., Koenigs, M., 2015. Ventromedial prefrontal cortex is critical for the regulation of amygdala activity in humans. Biol. Psychiatry 77, 276–284.
Nagai, Y., Critchley, H.D., Featherstone, E., Trimble, M.R., Dolan, R.J., 2004. Activity in ventromedial prefrontal cortex covaries with sympathetic skin conductance level: a physiological account of a "default mode" of brain function. Neuroimage 22, 243–251.
Noonan, M.P., Kolling, N., Walton, M.E., Rushworth, M.F., 2012. Re-evaluating the role of the orbitofrontal cortex in reward and reinforcement. Eur. J. Neurosci. 35, 997–1010.
Ochsner, K.N., Gross, J.J., 2008. Cognitive emotion regulation: insights from social cognitive and affective neuroscience. Curr. Dir. Psychol. Sci. 17, 153–158.
O'Reilly, J.X., Schuffelgen, U., Cuell, S.F., Behrens, T.E., Mars, R.B., Rushworth, M.F., 2013. Dissociable effects of surprise and model update in parietal and anterior cingulate cortex. Proc. Natl. Acad. Sci. U. S. A. 110, E3660–E3669.
Partala, T., Surakka, V., 2003. Pupil size variation as an indication of affective processing. Int. J. Hum. Comput. Stud. 59, 185–198.
Penny, W.D., Stephan, K.E., Mechelli, A., Friston, K.J., 2004. Modelling functional integration: a comparison of structural equation and dynamic causal models. Neuroimage 23 (Suppl. 1), S264–274.
Pessoa, L., 2009. How do emotion and motivation direct executive control? Trends Cogn. Sci. 13, 160–166.
Phelps, E.A., Delgado, M.R., Nearing, K.I., LeDoux, J.E., 2004. Extinction learning in humans: role of the amygdala and vmPFC. Neuron 43, 897–905.
Poldrack, R.A., 2012. The future of fMRI in cognitive neuroscience. Neuroimage 62, 1216–1220.
Power, J.D., Barnes, K.A., Snyder, A.Z., Schlaggar, B.L., Petersen, S.E., 2012. Spurious but systematic correlations in functional connectivity MRI networks arise from subject motion. Neuroimage 59, 2142–2154.
Power, J.D., Schlaggar, B.L., Petersen, S.E., 2015. Recent progress and outstanding issues in motion correction in resting state fMRI. Neuroimage 105, 536–551.
Preuschoff, K., Hart, B.M., Einhauser, W., 2011. Pupil dilation signals surprise: evidence for Noradrenaline's role in decision making. Front. Neurosci. 5, 115.
Pujara, M.S., Philippi, C.L., Motzkin, J.C., Baskaya, M.K., Koenigs, M., 2016. Ventromedial prefrontal cortex damage is associated with decreased ventral striatum volume and response to reward. J. Neurosci. 36, 5047–5054.
Quirk, G.J., Gehlert, D.R., 2003. Inhibition of the amygdala: key to pathological states? Ann. N. Y. Acad. Sci. 985, 263–272.
Rosa, M.J., Friston, K., Penny, W., 2012. Post-hoc selection of dynamic causal models. J. Neurosci. Methods 208, 66–78.
Rudebeck, P.H., Saunders, R.C., Prescott, A.T., Chau, L.S., Murray, E.A., 2013. Prefrontal mechanisms of behavioral flexibility, emotion regulation and value updating. Nat. Neurosci. 16, 1140–1145.
Russchen, F.T., Bakst, I., Amaral, D.G., Price, J.L., 1985. The amygdalostriatal projections in the monkey. An anterograde tracing study. Brain Res. 329, 241–257.
Salzman, C.D., Fusi, S., 2010. Emotion, cognition, and mental state representation in amygdala and prefrontal cortex. Annu. Rev. Neurosci. 33, 173–202.
Satterthwaite, T.D., Elliott, M.A., Gerraty, R.T., Ruparel, K., Loughead, J., Calkins, M.E., Eickhoff, S.B., Hakonarson, H., Gur, R.C., Gur, R.E., Wolf, D.H., 2013. An improved framework for confound regression and filtering for control of motion artifact in the preprocessing of resting-state functional connectivity data. Neuroimage 64, 240–256.
Schneider, B., Koenigs, M., 2017. Human lesion studies of ventromedial prefrontal cortex. Neuropsychologia 107, 84–93.
Sesack, S.R., Deutch, A.Y., Roth, R.H., Bunney, B.S., 1989. Topographical organization of the efferent projections of the medial prefrontal cortex in the rat: an anterograde tract-tracing study with Phaseolus vulgaris leucoagglutinin. J. Comp. Neurol. 290, 213–242.
Sokolov, A.A., Zeidman, P., Erb, M., Ryvlin, P., Pavlova, M.A., Friston, K.J., 2019. Linking structural and effective brain connectivity: structurally informed Parametric Empirical Bayes (si-PEB). Brain Struct. Funct. 224, 205–217.
Stephan, K.E., Penny, W.D., Moran, R.J., den Ouden, H.E., Daunizeau, J., Friston, K.J., 2010. Ten simple rules for dynamic causal modeling. Neuroimage 49, 3099–3109.
Stephan, K.E., Tittgemeyer, M., Knosche, T.R., Moran, R.J., Friston, K.J., 2009. Tractography-based priors for dynamic causal models. Neuroimage 47, 1628–1638.
Tsuchida, A., Doll, B.B., Fellows, L.K., 2010. Beyond reversal: a critical role for human orbitofrontal cortex in flexible learning from probabilistic feedback. J. Neurosci. 30, 16868–16875.
Tzourio-Mazoyer, N., Landeau, B., Papathanassiou, D., Crivello, F., Etard, O., Delcroix, N., Mazoyer, B., Joliot, M., 2002. Automated anatomical labeling of activations in SPM using a macroscopic anatomical parcellation of the MNI MRI single-subject brain. Neuroimage 15, 273–289.
Urry, H.L., van Reekum, C.M., Johnstone, T., Kalin, N.H., Thurow, M.E., Schaefer, H.S., Jackson, C.A., Frye, C.J., Greischar, L.L., Alexander, A.L., Davidson, R.J., 2006. Amygdala and ventromedial prefrontal cortex are inversely coupled during regulation of negative affect and predict the diurnal pattern of cortisol secretion among older adults. J. Neurosci. 26, 4415–4425.
van Reekum, C.M., Urry, H.L., Johnstone, T., Thurow, M.E., Frye, C.J., Jackson, C.A., Schaefer, H.S., Alexander, A.L., Davidson, R.J., 2007. Individual differences in amygdala and ventromedial prefrontal cortex activity are associated with evaluation speed and psychological well-being. J. Cogn. Neurosci. 19, 237–248.
Watanabe, N., Bhanji, J.P., Ohira, H., Delgado, M.R., 2019. Reward-driven arousal impacts preparation to perform a task via amygdala-caudate mechanisms. Cerebr. Cortex 29 (7), 3010–3022.
Yerkes, R.M., Dodson, J.D., 1908. The relation of strength of stimulus to rapidity of habit-formation. J. Comp. Neurol. 18, 459–482.
Zhang, S., Hu, S., Chao, H.H., Ide, J.S., Luo, X., Farr, O.M., Li, C.S., 2014. Ventromedial prefrontal cortex and the regulation of physiological arousal. Soc. Cogn. Affect. Neurosci. 9, 900–908.